THE STATUS OF STUDIES ON FAST REACTOR CORE THERMAL HYDRAULICS AT PNC

M. NISHIMURA, H. OHSHIMA, H. KAMIDE,
K. YAMAGUCHI, A. YAMAGUCHI
O-arai Engineering Center,
Power Reactor and Nuclear Fuel Development Corporation,
O-arai, Ibaraki-ken, Japan

ABSTRACT

An outlook was addressed on investigative activities of the fast reactor core thermal-hydraulics at Power Reactor and Nuclear Fuel Development Corporation. Firstly, a computational modeling to predict flow field under natural circulation decay heat removal condition using multi-dimensional codes and its validation were presented. The validation was carried out through calculations of sodium experiments on an inter-subassembly heat transfer, a transient from forced to natural circulation and an inter-wrapper flow. Secondly, experimental and computational studies were expressed on local blockage with porous media in a fuel subassembly. Lastly, information was presented on an advanced computational code based on a subchannel analysis code. The code is under the development and extended to perform whole core simulation.

1. INTRODUCTION

An overview is presented in this paper on fast reactor core thermal-hydraulic research and development of numerical analysis methods at Power Reactor and Nuclear Fuel Development Corporation (PNC). A natural circulation decay heat removal (NCDHR) has been one of the most important issues in this R&D field. Some computational models for a 3-dimensional code have been developed to predict the core thermal-hydraulic characteristics under NCDHR conditions accurately. The development was carried out in two stages: modeling for 1) thermal-hydraulics in the subassembly[1] and 2)thermal-hydraulic interaction between inside and outside the subassembly. The code was validated through the analysis of the sodium experiments: 61-pin subassembly steady state tests, unsteady 7-subassembly sodium tests under the transitions from forced to natural circulation with/without the inter-subassembly heat transfer and steady state test on the inter-wrapper flow (convection in the gap region between the subassemblies).

A local blockage with porous media at certain subchannels inside the subassembly brings another main thermal-hydraulic issue in which the maximum cladding temperature and its appearing position are of interests. A water test with magnified, 5/1 scale, 4 subchannel bare rod bundle model has been performed and its 3-dimensional thermal-hydraulic simulation model was developed. The computational result gave insights on the flow pattern and cooling mechanism inside the porous blockage and the interaction between the blockage inside/outside flows. Sodium and water tests with 1/1 scale 37-pin subassemblies have been also performed on the local blockage. These tests pay attention on corner blockage in which two rows of subchannels were blocked by the porous media from the inner face of one side wall of the wrapper tube. Preliminarily sodium test results were obtained. And flow visualization of the water test have been performed. Some calculations using subchannel analysis code ASFRE[2] were carried out for the sodium test to predict the maximum temperature and its appearing position.

Some advanced codes for the core thermal-hydraulics are under the development. ASFER is extended to the whole core thermal-hydraulic code ACT. To calculate detailed flow field in the subchannel of the wire wrapped rod bundles, a finite element method code is also developed.

All the data from the sodium and the water experiments were used for the validations of analysis codes to develop them capable of predicting thermal-hydraulics in the real reactor.

2. NATURAL CIRCULATION DECAY HEAT REMOVAL

2.1 Development of computational model for multi-dimensional codes

2.1.1 Subassembly thermal-hydraulics

The prediction of temperature distribution in the fuel subassembly is one of the most important issues for the reactor safety assessment. Temperature distributions thus the maximum cladding temperature in the subassemblies are interactively affected by inter-subassembly heat transfer and cooling capability of an inter-wrapper flow. The inter-subchannel mixing, which is caused by wire sweeps, turbulence, and thermal plumes due to heating, is one of the most important parameters predominating temperature profiles inside the subassembly. A systematically formulated mixing correlation was constructed at MIT for the subchannel analysis to apply to all flow regimes[3],[4].

Cheng and Todreas[3] reported that under the forced convection, the mixing due to swirl flows generated by wrapped wire spacers on the pins plays key role. While the mixing induced by thermal plumes prevails, in the mixed convection flow regime. And the inter-subchannel mixing plays minor role under the natural convection condition. Because an inter-subchannel flow redistribution is predominant in determining temperature profiles inside the subassemblies. From these contexts, a threshold function was proposed to control the usage of mixing factor and enabled simulations to handle the all flow regimes continuously; forced, mixed and natural convection, appeared in the reactor transient conditions. A detailed expression of this modeling is presented in Ref.[1]. This modeling for effective diffusivity was implemented to the diffusion terms of the conservation equations in the multi-dimensional thermal hydraulic code AQUA[5]. The computational models and the code were validated through the analyses of a sodium experiments.

2.1.2 Thermal-hydraulic interactions between flows inside and outside the subassembly

The inter-wrapper flow (IWF) occurred in NCDHR is a flow of cold coolant fluid comes from direct heat exchanger (DHX) immersed into a hot plenum[6]. It penetrates into the gap regions between the subassemblies (inter-wrapper gaps) cooling the subassemblies from outside of the wrapper tube wall. Two major influences have been concerned on the IWF: 1) temperature decrease inside the subassemblies and 2) decrease in natural circulation head within the primary loop. Of course the former is a positive effect and the latter is a negative one regarding the decay heat removal capacity.

Another type of the IWF was reported[7] which was observed under forced circulation conditions. This type of the IWF is occurred by the driving force from the pressure difference between the core outlet region just below the upper internal structure (UIS) and the hot plenum. Thus the coolant dives into inter-wrapper gaps within the center region of the core outlet, turns to horizontal direction crossing through the wrapper tube bundle, goes upward in the outer region of the core and exits from the inter-wrapper gaps into the upper plenum.

The IWF occurred in NCDHR has been mainly studied at PNC recently. In this case, an adequate modeling is of importance to treat the interactions between thermal-hydraulic fields inside and outside the subassembly. Inside the subassembly, a large difference of friction force exists between interior and edge subchannels which imposes velocity difference between them. This also makes temperature in the edge subchannels lower than subassembly bulk temperature. Therefore, edge subchannel temperature should be referred to as a characteristic temperature of flow inside the subassemblies to calculate heat fluxes through the wrapper wall tubes unless a specific correlation for heat transfer were used. A square mesh model of the subassemblies was proposed to simulate the IWF, flows inside the subassembly and the hot plenum simultaneously. The interior and edge subchannels had each own mesh in this arrangement. Typical mesh arrangement of this model is presented in *FIG. 1*. This mesh simulated the 7-subassembly sodium test facility: plant dynamics test loop with direct heat exchanger (PLANDTL-DHX, see *FIG. 5*). The detail of the test facility will be addressed later.

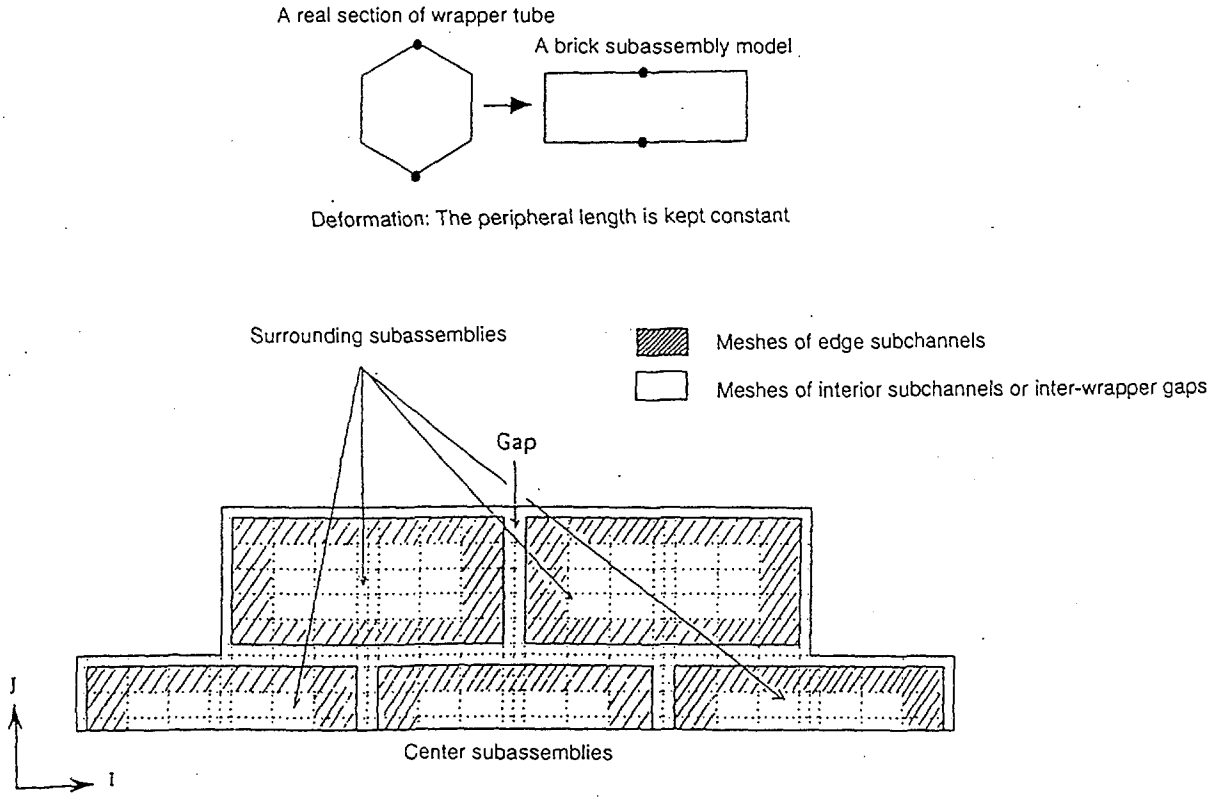

FIG. 1 Brick subassembly mesh arrangement

2.2 Validation through sodium experiments

2.2.1 Inter-subassembly heat transfer

Predictive capabilities of house code AQUA was examined on temperature profiles in the subassemblies accompanied by the inter-subassembly heat transfer. The code validation was carried out through calculations of sodium experiments: core component test loop (CCTL-CFR)[8] and PLANDTL-DHX. A schematic diagram of CCTL-CFR and its test section are shown in *FIG. 2*. TABLE 1 shows specifications of the test rigs simulated in the present code validation. The test section is consisted of a 61-pin bundle and two 19-pin bundles, simulating the blanket and driver subassemblies respectively. Each bundle is such bounded by solid steel slab to the others that the heat flux due to the inter-subassembly heat transfer is measurable using thermocouples enveded on the slab surfaces. A cooling channel was also equipped in 61-pin bundle behind the wrapper wall opposite to the 19-pin bundle side to provide various thermal boundary conditions simulating the inter-subassembly heat transfer.

Test conditions of CCTL-CFR used in the code validation were shown in TABLE 2. In Case-61A, the 61-pin bundle was heated by the 19-pin bundles and cooled by the cooling channel featuring heat flux crossing the 61-pin bundle. While the 61-pin bundle was under almost adiabatic wrapper wall condition in Case-61B. A staggered half pin mesh arrangement[9] were used to simulate the fuel pin bundles, in which each mesh accommodates only 1 subchannel in its horizontal cross section.

Comparisons of the experimental and numerical temperature distributions are shown in *FIG. 3* The difference of temperature between the experiment and the prediction is less than 3 °C that is within the uncertainties of the measurements. In Case-61A prediction reproduced temperature gradient imposed by the heat flux crossing the 61-pin bundle from 19-pin bundle side to the cooling channel.

2.2.2 Transient from forced to natural circulation

To simulate the complex phenomena in the reactor, a core model composed of seven subassemblies was installed in the sodium test loop PLANDTL-DHX. A schematic flow diagram of

PLANDTL-DHX is shown in *FIG. 4*. The core model's horizontal cross section is illustrated in *FIG. 5*, and TABLE 1 shows specifications of it. The core model was connected to the upper plenum in which DHX of a direct reactor auxiliary cooling system (DRACS) was immersed to remove the decay heat. The inter-wrapper gaps filled with sodium were also connected to the upper plenum. The primary circuit had an intermediate heat exchanger (IHX) equipped with a primary reactor auxiliary cooling system (PRACS), a pump, and a lower plenum. Sodium coolant flow was fed by three lines respectively to the center subassembly, the three surrounding subassemblies ranging in one side, and

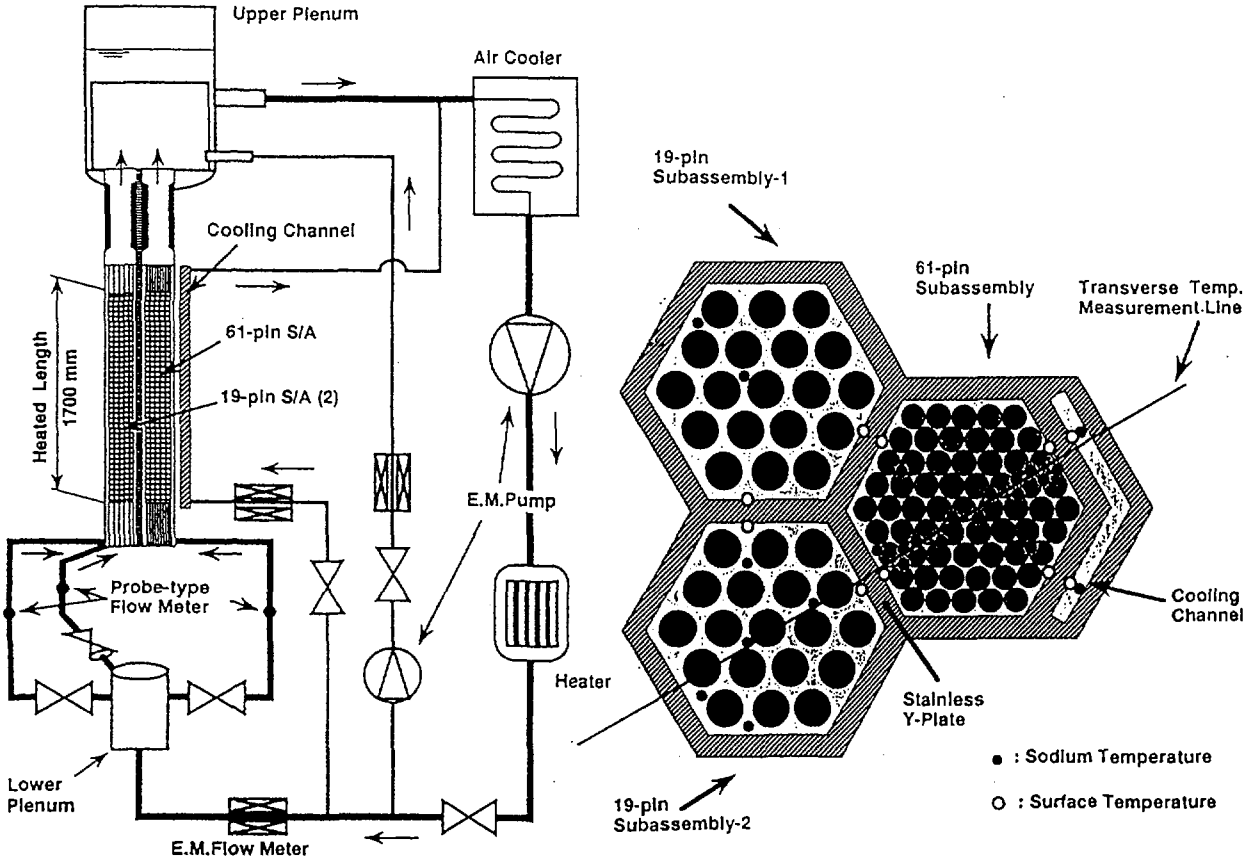

FIG. 2 Schematic diagram of core component test loop (CCTL-CFR) and its test section

TABLE 1 SPECIFICATIONS OF SODIUM TEST SUBASSEMBLIES

		CCTL-CFR		PLANDTL-DHX	
		Driver	Blanket	Center	Surrounding
Number of Subassemblies		1	2	1	6
Number of Pins		61	19	37	7
Pin Diameter	(mm)	16.0	25.0	8.3	20.8
Pin Pitch	(mm)	17.4	30.2	9.9	22.4
Spacer Wire Diameter	(mm)	1.4	5.2	1.5	1.5
Spacer Wire Lead	(mm)	200	700	165	165
Wrapper Tube Inner Flat to Flat Distance	(mm)	140.0		63.0	
Inter-wrapper Gap Width	(mm)	0		7	
Wrapper Tube Thickness	(mm)	15		4	
Heated Length	(mm)	1700		1000	
Axial Power Profile		Uniform		Chopped Cosine	

TABLE 2 TEST CONDITIONS OF CCTL-CFR

Case No.	Heater Power (KW/Ass.)		Flow Rate (ℓ/min/Ass.)			Inlet Temperature (℃)			Heat Transfer To 61pin Bundle
	61 pin Bundle	19 pin Bundle	61 pin Bundle	19 pin Bundle	COOLING CHANNEL	61 pin Bundle	19 pin Bundle	COOLING CHANNEL	
61A	14.5	33.5	10.3	13.1	1.0	251.3	252.1	247.2	heated
61B	15.3	7.8	29.4	13.5	0.0	251.2	252.2	-	isothermal

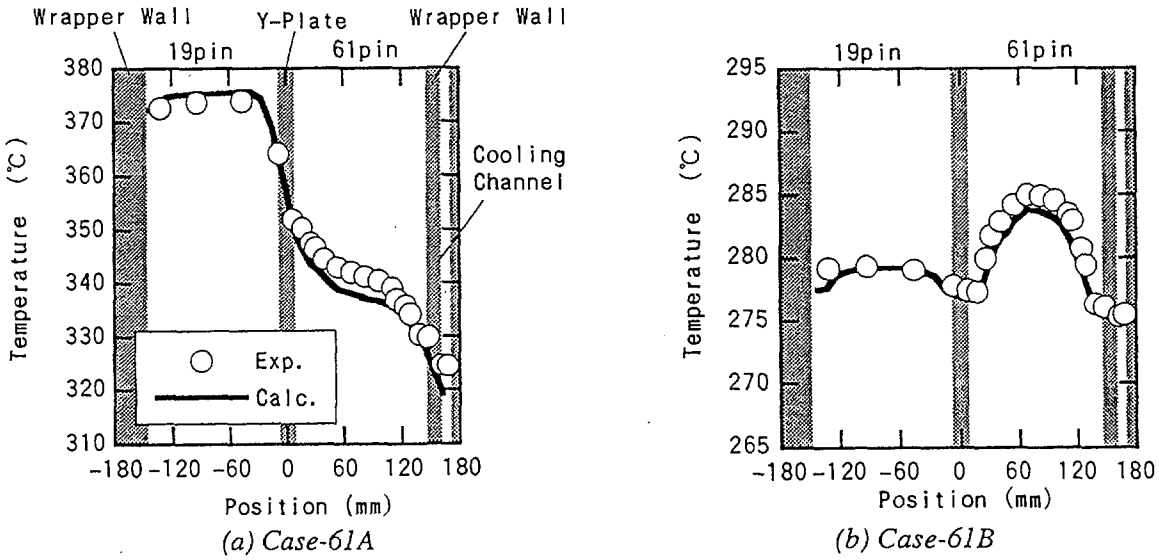

FIG.3 Comparisons of temperature profiles in CCTL-CFR

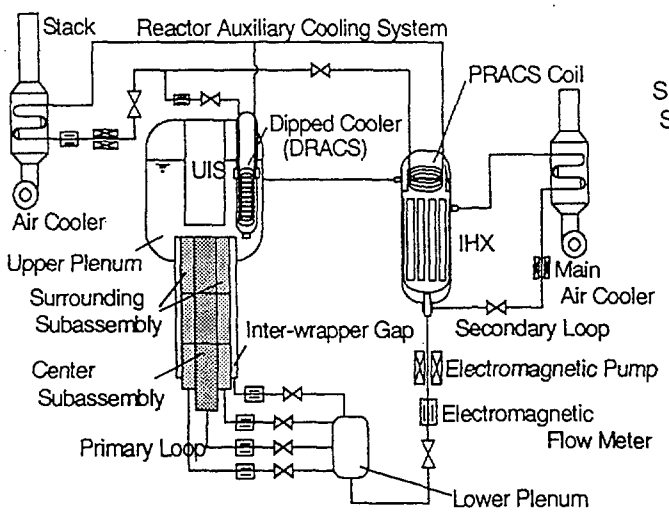

FIG. 4 Flow diagram of PLANDTL-DHX

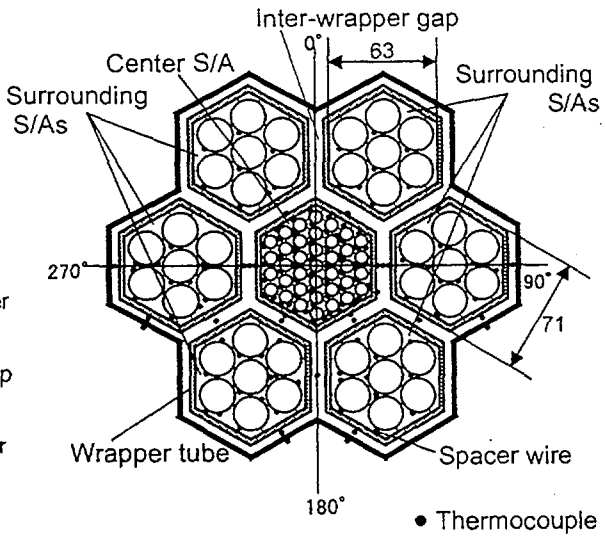

FIG.5 Horizontal cross section of the core model

the opposite side. The flow rate in each line of the three was controlled individually. The secondary circuits of the IHX and the two reactor auxiliary cooling systems had air coolers and pumps. This facility could simulate transitions from forced to NCDHR conditions in the primary and decay heat removal systems of FBRs.

The center subassembly consisted of a 37-pin bundle. And the surrounding subassemblies had 7 pin bundles in each. Every pin was heated by electrical heater. The heater pin in the center subassembly simulated a core fuel pin of a FBR in full scale. The flat to flat distance of the subassembly was about 1/2 of that of FBRs which contains 217 or 271 fuel pins. Coolant temperatures of the core model were measured by K-type thermocouples of 0.3 or 0.5 mm in diameter. The positions of thermocouples were also shown in *FIG. 5*. The signal of temperature, flow rate, and electric power of heater pins were recorded at a sampling interval of 0.096 s using a mini-computer system.

Symmetry with respect to the vertical center plane (parallel to 90°-270° line, see *FIG. 5*) of the core model was assumed on the thermal hydraulic field regarding the geometry and the boundary conditions. Again the staggered half pin mesh arrangement was applied to the core model of PLANDTL-DHX. In vertical direction, each subassembly was divided into 29 meshes for the total length of 2825 mm. And the mesh widths in the heated length were 82.5 mm or 87.5 mm. The sodium coolant in the inter-wrapper gaps were assumed to be stagnant in the calculations.

Transient behaviors in the multi subassemblies were studied under the conditions with and without inter-subassembly heat transfer. In the experiment of Case-TR43, a transient condition was given as follows. Initially, the facility was operated at 12% power and forced flow velocity corresponding to the rated condition of the real reactor. Then scram shutdown was imposed to reach 2% forced flow rate which simulated the NCDHR condition. Time trends of power and flow rates are shown in *FIG. 6*. During the transition, the flow rates and the heater powers in the all subassemblies were controlled to kept identical with each other. In this condition, therefore, no inter-subassembly heat transfer could occur.

IHX was used as a heat sink of the primary system to suppress the IWF. The IWF is also suppressed if the PRACS were applied as a heat sink. Therefore, the experiments mentioned below were characterizing NCDHR with IHXs or PRACSs.

In Case-TR49, all test conditions were set similar to that of Case-TR43 except the initial heater powers of the surrounding subassemblies. They were set lower than the center subassembly to make the surroundings outlet temperature lower by 30 °C than the center if adiabatic wrapper walls were assumed. Thus the inter-subassembly heat transfers occurred in Case-TR49.

Time trend of temperature variations are presented in *FIG. 7* at the center subchannel in the center subassembly where peak temperatures were observed. The maximum temperatures in space and time were observed at the top end of the heated section and around 150 s. in both cases. The numerical results over-predicted the maximum temperatures by 15 to 20 °C. Overall, the calculations showed good agreement with the experiments.

Figure 8 shows variations of horizontal temperature profiles at the top end of the heated section. In both cases, the prediction reproduced the change of temperature profiles well. At the start of the scram (t = 0 s), the predicted and the experimental temperature profiles are in good agreement in both cases .

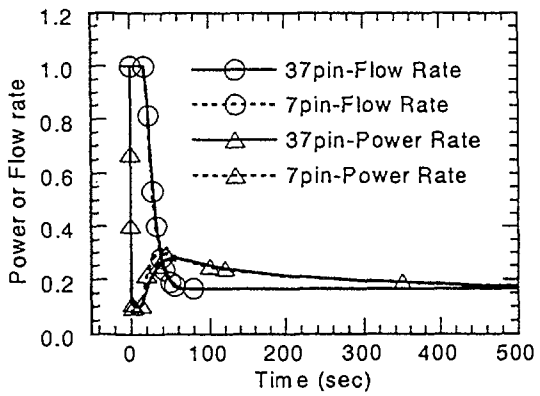

FIG. 6 Power and flow rate time trend of transition experiments

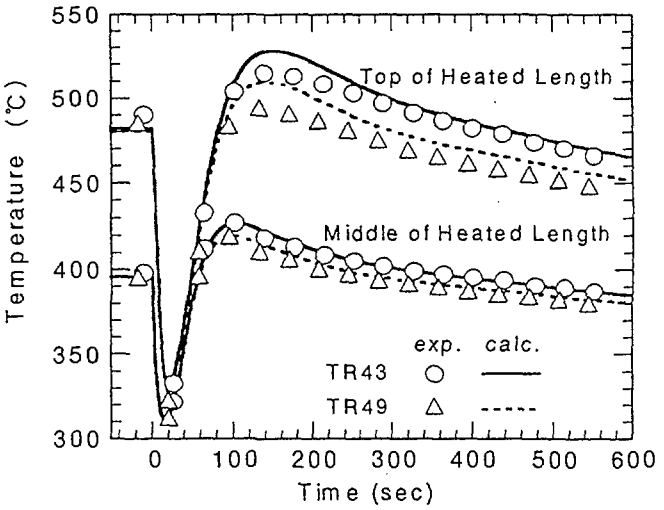

FIG.7 Time trend of temperature variations at the center subchannel in the center subassembly

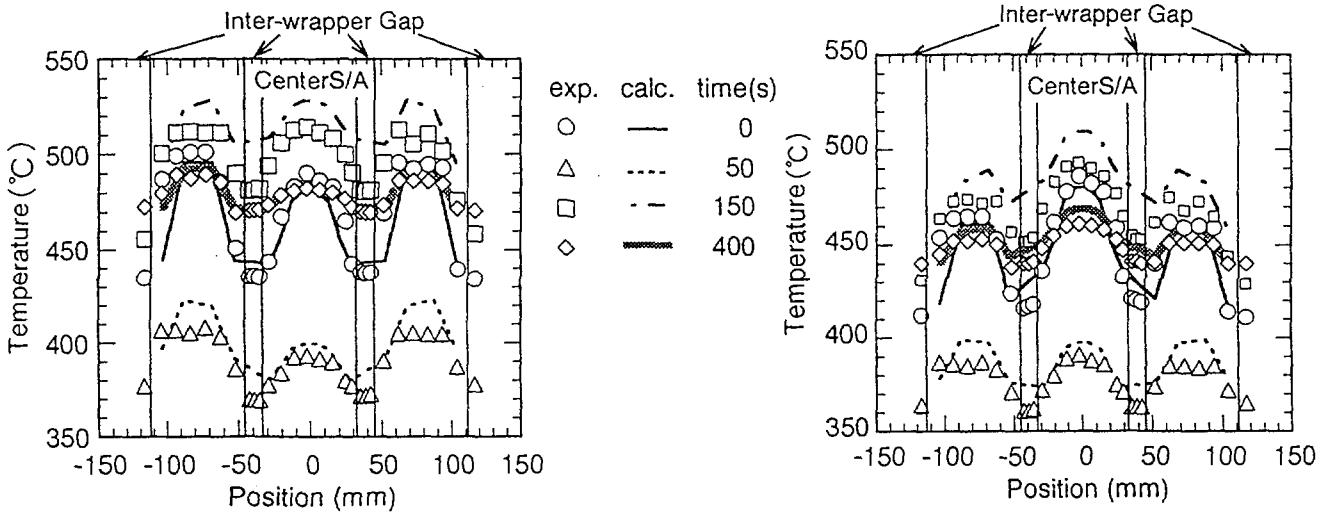

(a) Iso-temperature rise (Case-TR43) *(b) Inter-subassembly heat transfer (Case-TR49)*

FIG. 8 Variation of horizontal temperature profiles at the top end of the heated section

After 50 s from the scram, predicted temperatures were 15 to 20 °C higher than the experiments in the surrounding subassemblies. And at 150 s of both cases, the predicted maximum temperatures were over-estimated by 15 to 20 °C both in the center and the surrounding subassemblies. Temperatures in the inter-wrapper gaps also gave large deviation between the predictions and the experiments. This deviation caused the over-prediction of the maximum temperature. In the calculations, sodium in the inter-wrapper gaps was assumed to be stagnant. Although, these experimental results suggest existence of cooling effect by the IWF which was neglected in the calculations. Actually, temperature differences about 25 °C are seen between the center and outer inter-wrapper gaps at 150 s in both cases. These temperature differences may cause the IWF in reality. At 400 s, the predictions gave good agreements with the experiments of both cases.

2.2.3 Inter-wrapper flow

Some tests were performed on the IWF using PLANDTL-DHX. During first stage of the scram, i.e. the fast transient period, the IWF would show slight cooling effect as seen in the above transient tests. The cooling effect of the IWF becomes more active after the hot plenum is cooled by DHXs. Because cold coolant from the DHX penetrates into the inter-wrapper gaps. Therefore, it is important to clarify behavior of the IWF after the hot plenum is cooled: in general 1000 s after the scram and

essentially under quasi-steady states. From this point of view, we carried out the sodium test under the steady states. The 7 subassemblies were set to provide the same heater power. The DRACS removed all the thermal energy generated by the heaters except heat loss which was about 5 % of the total heater power. The test condition is listed in TABLE 3. The sampling time and its interval of temperature data acquisition were 180 s and 0.096 s respectively.

TABLE 3 CONDITIONS OF TESTS ON THE INTER-WRAPPER FLOW

Case No.	Power		Flow Rate		Inlet Temperature	Heat Sink in the Primary Loop
	(kW)	(%)	(ℓ/min/Ass.)	(%)		
I10	18.38	1.53	4.15	1.04	277.4	DHX
I05	18.38	1.52	2.06	0.52	301.9	DHX

A sector model of 180 ° was used in the calculation based on the assumption of flow field symmetry regarding geometry and boundary condition of the test section. The computational region took 7-subassembly core model and the hot plenum into account. Five of seven subassemblies were simulated by the square shaped model with their full length (see *FIG. 1*). The cross section of a subassembly was such modeled that the peripheral length of a rectangle wrapper wall in the numerical model was set equal to that of the hexagonal wrapper tube of the test rig, to simulate the heat transfer area and relative position of the subassemblies. The all subassemblies were thermally connected to the inter-wrapper gaps using the thermal structure model. In the hot plenum, the following components were modeled: DHX, UIS and outlet nozzle. For inlet boundary conditions of the primary system, the flow rate and the temperature were set at the pin bundle inlet of the subassemblies. In the DHX model, the flow rate and the inlet temperature of the secondary (i.e. auxiliary) system were provided as boundary conditions. The test condition calculated here corresponded to natural circulation flow regime. And inter-subchannel mixing plays so minor role in this flow regime, as mentioned in section 2.1.1, that no mixing correlation was used in this calculation.

Velocity fields in the vertical section of the inter-wrapper gaps are shown in *FIG. 9*. In the case of 0.5% flow rate (Case-I05), the cold coolant dived into the core barrel from the right side, went down, turned, went up and out to the hot plenum at the left side. While flow direction was entirely opposite in Case-I10. Temperature field in the core barrel was colder at the upper part and hotter at the lower part, when the IWF occurred. In such a temperature field, specific weight field of the fluid is so unstable that axially symmetrical flow was hard to be occurred unless an adequate flow shroud were installed, even the initial boundary condition was axially symmetrical. And flow direction could not be

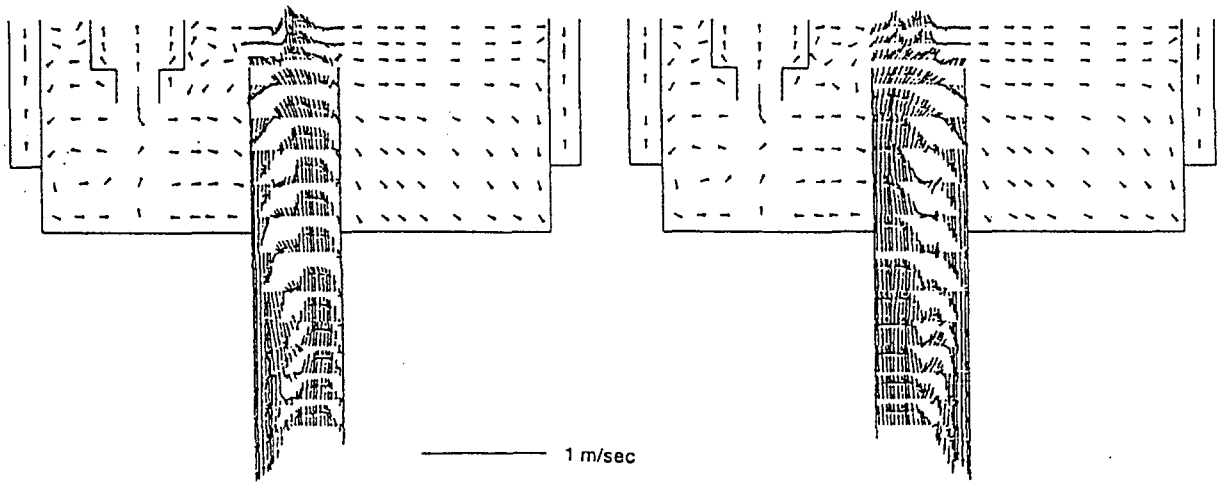

(a) Case-I10 : 1% flow rate *(b) CaseI05 : 0.5% flow rate*

FIG. 9 Velocity fields in the vertical section of the inter-wrapper gaps

reproduced deterministically. Figure 10 presents velocity fields in the region including the heated section. In both cases, reverse and recirculating flows were occurred inside the subassembly at the diving side of the IWF. The recirculating flow was lager in lower flow rate case. Diving depth and velocity of the IWFs were almost same in both cases. A comparison of axial temperature profile along the center subchannel in the center subassembly are shown in *FIG. 11*. Numerical data agreed well to the experiment in Case-I10. While the computation over-predicted the temperature especially in the upper part of the subassembly in Case-I05, invalidating predicted heat removal capability of the IWF. Horizontal temperature profiles at the top end of the heated section is presented in *FIG. 12*. The calculations reproduced overall features of the temperature profiles. In Case-I10, the experimental temperature was traced well by the prediction in the center subassembly. The experimental and numerical data showed differences in the outer subassemblies. However if the numerical data plots in the right and left sides of the outer subassemblies were changed, they showed fairly good agreement. In Case-I05, numerical data over-predicted the temperature. The maximum difference was seen at the left side inter-wrapper gap. This result may imply invalidity of assumption of the vertical symmetrical plane including 90° -270° line. The test section had another symmetrical plane in 120°-300° direction. Further more, in such an unstable flow field, no symmetrical plane could be expected. Therefore, strictly speaking, the IWF is essentially 3-dimensional and unsteady. This suggests the need for a time-dependent computation of full-sector core.

3. LOCAL FAULT WITH POROUS BLOCKAGES

3.1 Evaluation methods and experimental program

Local blockage issue in the subassembly is one of the most important issue of safety assessments for the fast reactor. An experimental program is under going in PNC to establish the evaluation methods for the local fault issue. The porous type blockage is assumed in the program as the most certain form of the blockage in the wire wrapped pin bundle geometry.

Computational methods have been developed to evaluate the highest temperature in the blocked subassembly. Integrity of the subassembly or the fuel pin depends strongly on the highest temperature of the structures. Two methods were developed to cover the phenomena in a subchannel scale and in a subassembly scale.

The subchannel scale phenomena inside/outside the porous blockage were calculated by a three-dimensional thermal-hydraulic analysis code, CASCADE. In the code, three-dimensional thermal conduction in a porous structure was modeled. Flow through the porous structure and heat transfer among coolant fluid, fuel pins, and porous structure were taken into account in the porous-body model.

Whole subassembly analysis was performed by an subchannel analysis code, ASFRE. It would predict the highest temperature in a blocked subassembly under actual reactor conditions. In the code, the porous blockage was also calculated by a physical model using lumped parameters of the subchannel scale, for example, an effective heat conduction coefficient. Such lumped parameters were derived from fine mesh calculations using the CASCADE code.

In the experimental program, three kinds of tests were planned in order to investigate the phenomena in a subchannel scale and in a subassembly scale. These were 4-subchannel water test, 37-pin water test, and 37-pin sodium test.

The 4-subchannel water test were carried out as a fundamental experiment to investigate the thermal-hydraulics in a porous blockage and also interaction between the inside/outside flows of the blockage. Schema of the test section is shown in *FIG. 13*. Spatial distributions of temperature and flow velocity in a porous blockage are of interests to establish a lumped model of the porous blockage and to validate the computational method of subchannel scale using the CASCADE code.

Two types of pin bundle geometry experiments were carried out using water and also sodium as working fluids. For the water and sodium experiments, the same geometry of 37-pin bundle was used. Flow field was measured in the water test. The velocity data are helpful to understand the phenomena in the sodium experiment which provides only the temperature data. These data are used to validate the subchannel analysis code, ASFRE and also the lump parameters of porous blockage.

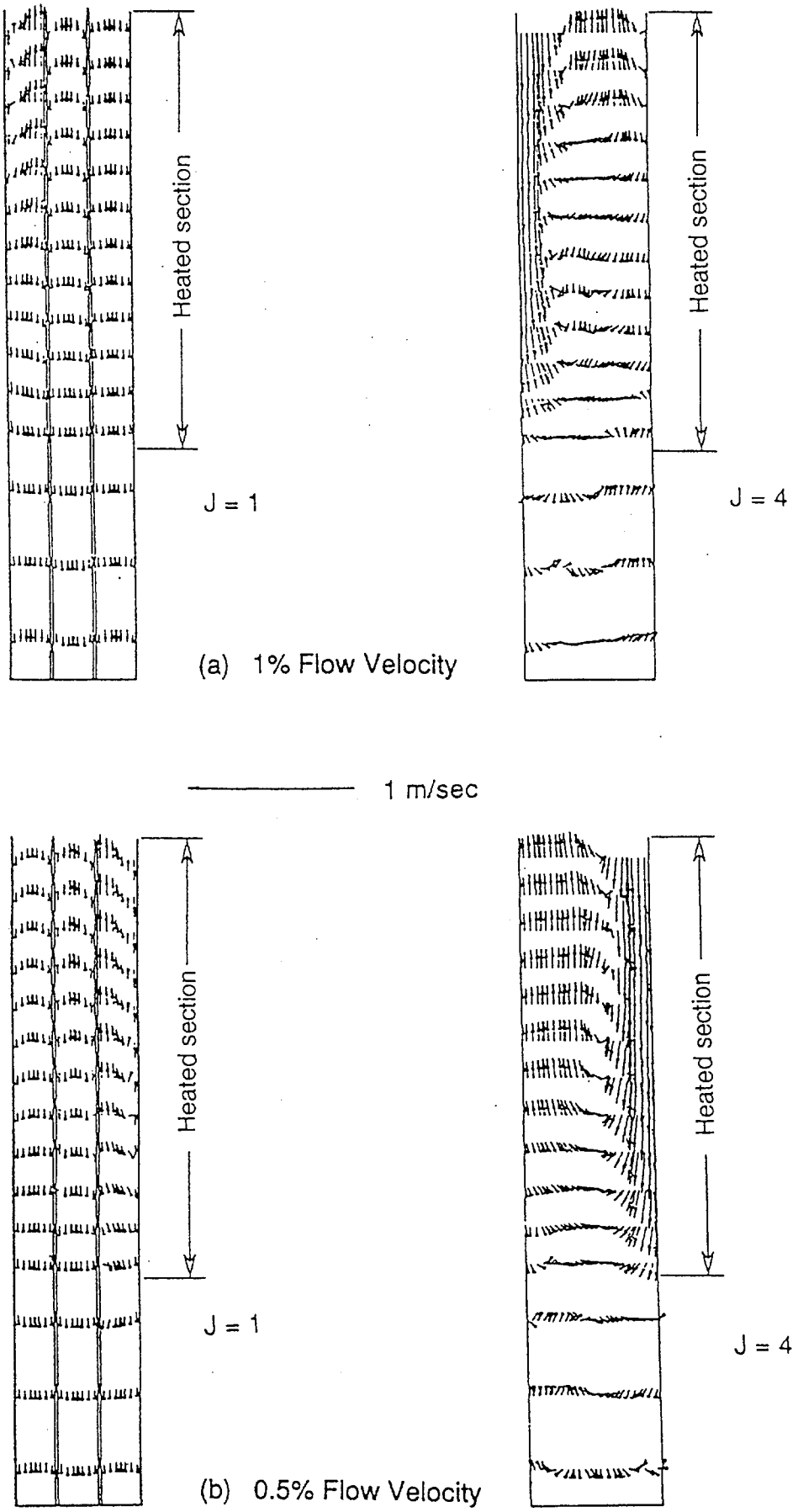

FIG. 10 Velocity fields in vertical planes at heated section of the core model

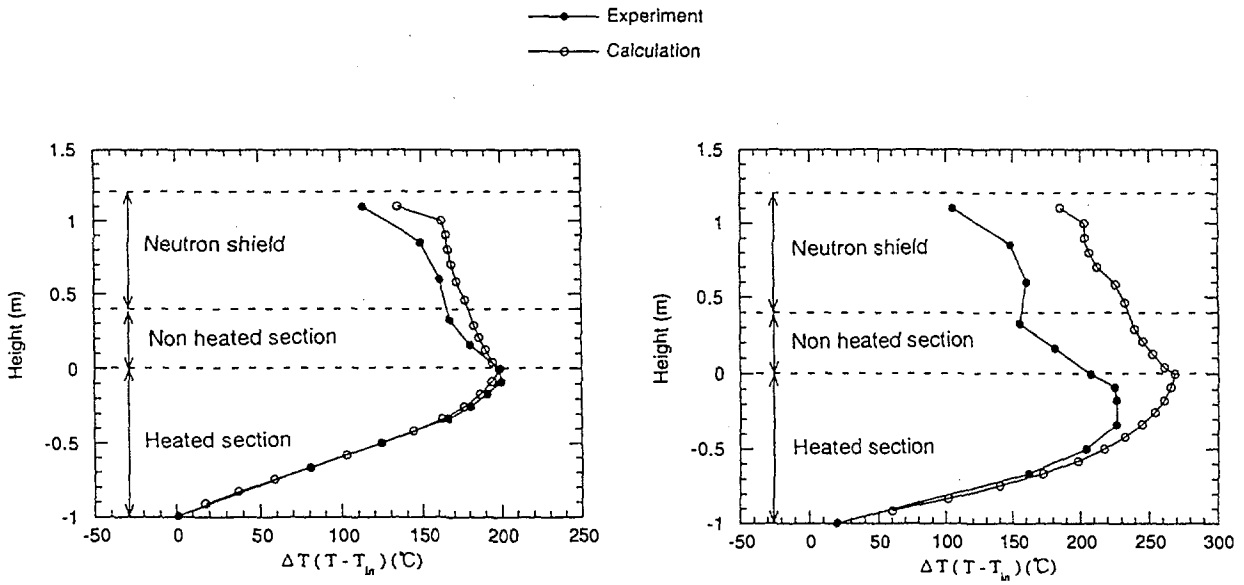

(a) Case-I10 : 1% flow rate *(b) CaseI05 : 0.5% flow rate*

FIG. 11 Comparisons of axial temperature profile along the center subchannel in the center subassembly

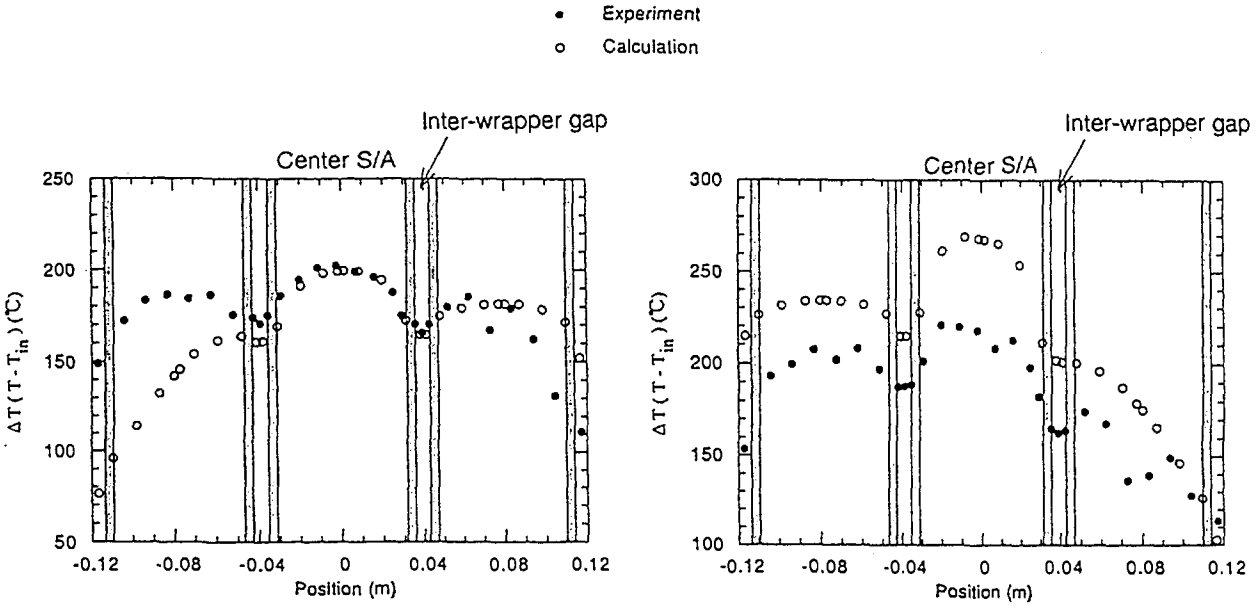

(a) Case-I10 : 1% flow rate *(b) CaseI05 : 0.5% flow rate*

FIG. 12 Horizontal temperature profiles at the top end of the heated section

3.2 Fundamental experiment

Velocity measurements in the unplugged subchannel and temperature measurements of the coolant inside/outside the blockage were made. Particular interest was the correlation between the temperature inside/outside the blockage and the flow field outside the blockage, thus revealing the heat transfer mechanism within the blockage.

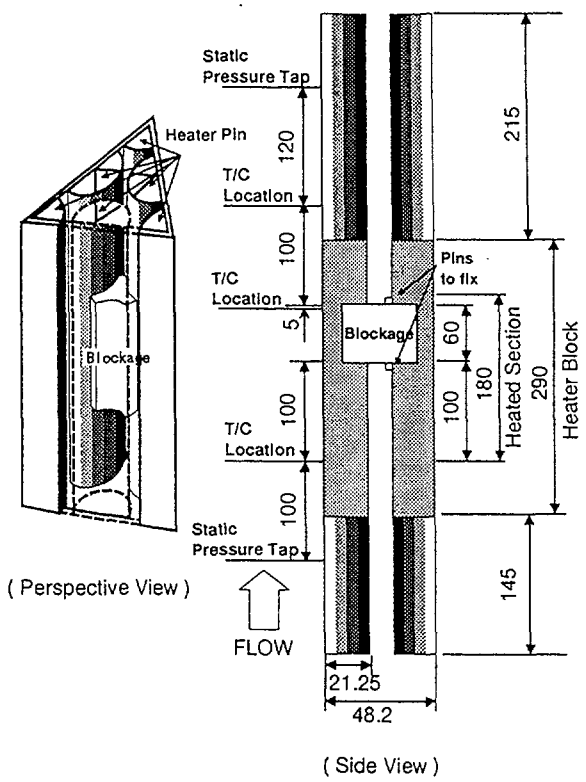

FIG. 13 Schematic view of 4-subchannel test section

In parallel, a multi-dimensional analysis modeling with CASCADE code has been developed to predict the hottest point and the maximum temperature in the subassembly. The porous blockage was modeled with porous body model introducing a volume porosity and a surface permeability of the fluid. A thermal structure model was used to calculate the heat transfer among the heater pins, the blockage and the coolant fluid. The interaction of heat transfer among these structures and the fluid was calculated by empirical correlations of wall-particles, wall-fluid, particles-fluid, and equivalent thermal conductivity of the fluid in the porous media. Turbulent and laminar calculations, i.e. calculations with and without k-ε two equation turbulence model were performed.

Comparisons of the horizontal temperature profiles are shown in *FIG. 14.* In the lower part of the blockage, the laminar calculation showed better agreement with the experiment than the turbulent one. While the turbulent calculation gave better result in the upper part. Figure 15 presents predicted distributions of temperature and flow patterns inside the porous blockage. One can see an injection into the porous media at the bottom plane. On the right hand side plane facing to the unplugged subchannel, a suction occurred in the half lower portion, and a small injection region was seen just above the suction part. Only vertical upward flow was occurred at the left hand side plane facing to the heater pin surface. The position of the maximum temperature was observed on the heater pin surface and in the blockage region. This position of hottest point implied influences of cooling due to the horizontal velocity component inside the porous media. Because temperature should rise monotonously with rise in level if only the upward axial velocity component existed. The importance of horizontal flows on the cooling was also confirmed experimentally[10]. The multi-dimensional analysis provide useful information to understand thermal-hydraulic interactions inside/outside the blockage. Nevertheless the present modeling needs more brush up in quantitative predictive capability.

3.3 Experiments with 37-pin bundles

Evaluations under the actual reactor conditions will be performed by the subchannel analyses. To validate such simulation method, pin bundle geometry experiments were planned using water and sodium as working fluids and the identical geometry of 37-pin bundle. The porous blockage is set at

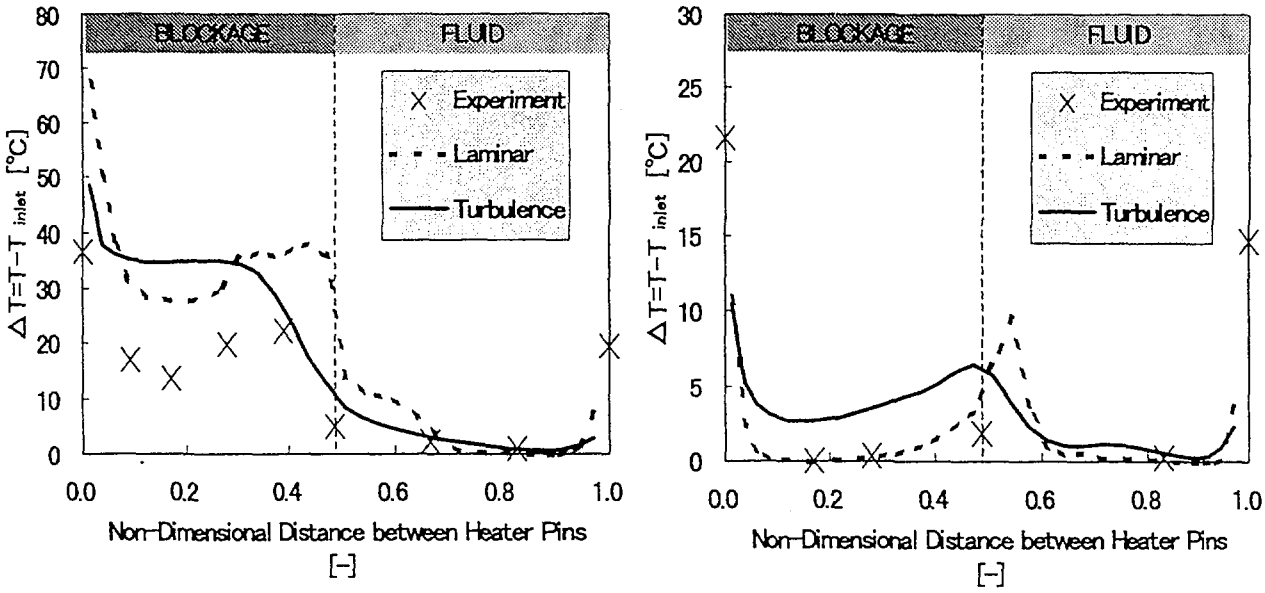

(a) Upper thermocouple location *(b) Lower thermocouple location*

FIG. 14 Comparisons of horizontal temperature profiles in 4-subchannel model

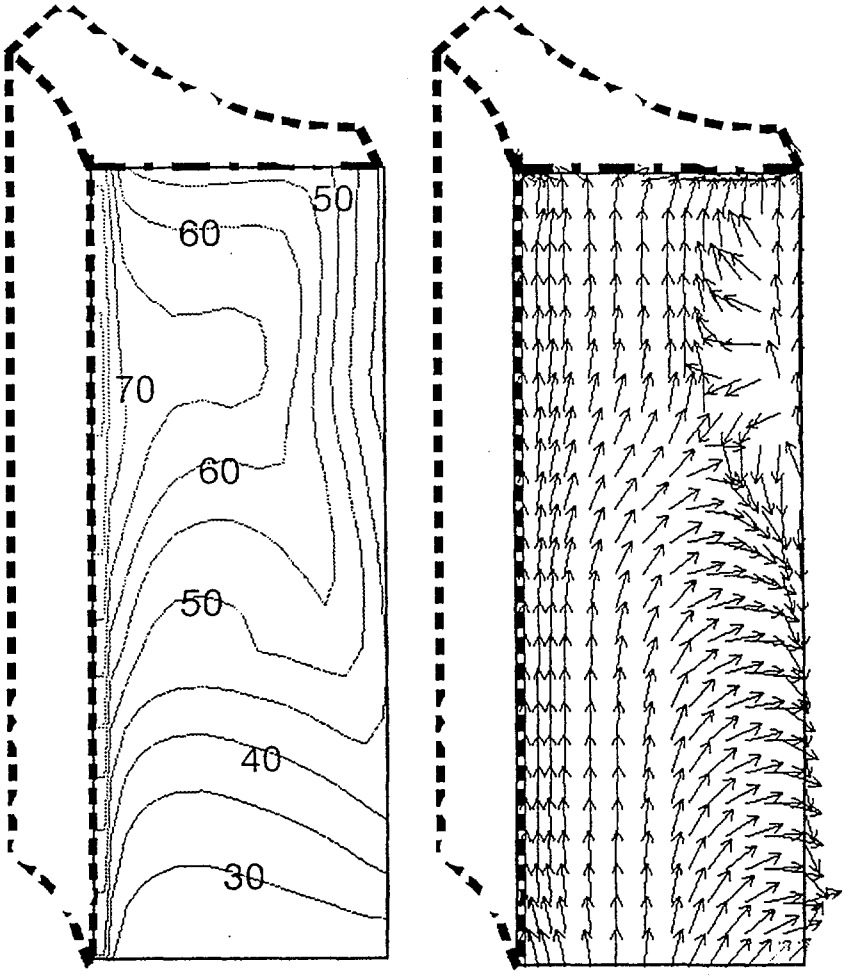

(degree centigrade) *(allows show direction only)*

(a) Contour of iso-therms *(b) Flow directions*

FIG. 15 Predicted temperature distribution and flow patterns in the porous blockage (Calculated with turbulence model)

outer most two layers of subchannels along one side of hexagonal wrapper tube. Figure 16 shows schema of the test section of sodium test. This arrangement includes a blocked subchannel surrounded by three blocked subchannel, which will have the maximum temperature due to restricted flow paths to cool the blockage.

In the water test, flow fields are measured in the subassembly, especially around the blockage, for example, a recirculation flow region downstream of the blockage. The velocity data are measured by an two-dimensional laser Doppler anemometer and ultrasonic velocity profile monitor (UVP). For fine measurements of spatial dependency, two times enlarged model is used. Influences of swirl flow due to the wrapping wires are also of interests. The wrapping wires and the blockage can be removed from the test section. The experiments are under going. The velocity data will be useful to estimate the sodium experimental results and the code validation.

The sodium test is also under going using the identical geometry of the water test with the 1/1 scale of the Japanese demonstration reactor. The wrapping wires are simulated and heated length is 0.65 m with a flat power distribution. The porous blockage is set at middle level of the heated length. The temperatures at pin surfaces covered by the blockage and the center of blocked subchannels are measured at several heights in the blockage and also in the downstream region. The experimental parameters are heater power of the simulated fuel pins and sodium flow rate in the subassembly. Preliminary tests were carried out under low power conditions. The temperature profiles including the porous blockage were successfully measured. The calculation has predicted that the maximum temperature was yielded almost upper end of the blockage. And the temperature rise from the inlet to the maximum values was essentially proportional to the ratio of heater power to flow rate. These features were also observed in the preliminary experiments.

4. ADVANCED CODES FOR CORE THERMAL-HYDRAULICS

4.1 ASFRE and SPIRAL codes - fuel subassembly thermal-hydraulics

For the design of the FBR, it is necessary to evaluate the coolant thermal-hydraulic behavior in wire-wrapped fuel-pin bundles accurately under various operational and unusual conditions, e.g. forced to natural circulation, local blockage, deformed fuel pin and so on. The simulation of thermal-hydraulics in fuel subassemblies has been generally done by using mathematically expressed empirical correlations on the basis of model parameters, i.e. engineering model. They should be determined based on experiments that reflect actual geometry and thermal-hydraulic characteristics. However,

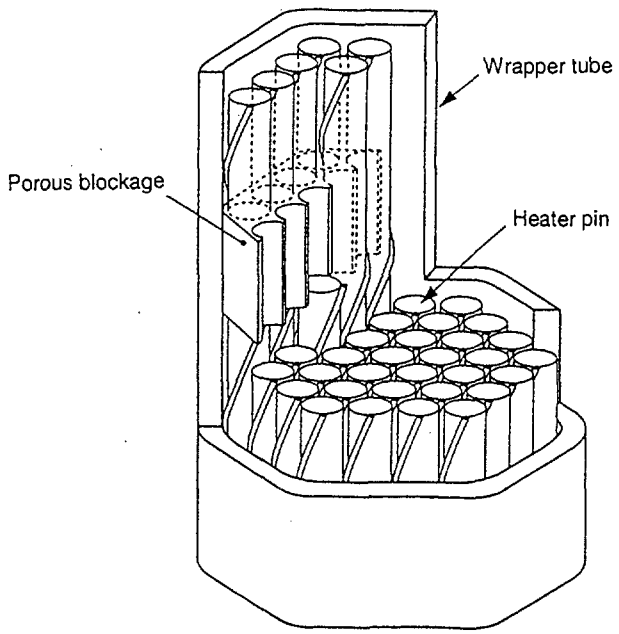

FIG. 16 Schematic test section of 37-pin sodium subassembly

measurement in sodium is not easy and the experimental cost is expensive. Direct numerical simulation could be an alternative way to determine the empirical correlation for the engineering model. From this viewpoint, two numerical methodologies are being developed and applied to the thermal-hydraulic simulation in the wire-wrapped fuel subassembly. One is a parametric method, i.e. a subchannel analysis code ASFRE that uses more empirical correlations in the physical modeling and that is applicable to large-scale fuel subassemblies such as 271-pin bundle. The other is a mechanistic numerical simulation, i.e. finite element analysis code SPIRAL that uses the least empirical correlations, if any. However, it is noted that the mechanistic approach is not feasible to solve whole 271-pin bundle fuel subassembly because of high computing cost. Therefore interactive use of the two approaches is a practical way.

ASFRE code is designed to calculate single-phase flow thermal-hydraulic phenomena in the fuel subassemblies, taking into account of the fuel pin heat conduction and heat transfer to the fluid. A triangular coordinate system is adopted in ASFRE to model the fuel bundle in accordance with the triangular pin array configuration. The finite difference equations of mass, momentum and energy conservation are derived using the standard control volume integration method based on a specific subchannel control volume. A large system of non-linear equations and the equation of state are solved based on the semi-implicit method developed Liles and Reed[11]. All equations are reduced to a set of the Newton-Raphson iteration equations in the form of a large and sparse matrix. The resulting pressure equation is solved by the Incomplete LU Decomposition Bi-Conjugate Gradient (ILUBCG) method[12]. Momentum or energy exchange between stationary solid wall and fluid and between fluids at subchannel boundaries are modeled in terms of rather simple correlations such as friction factor, wire forcing function, heat transfer coefficient, and turbulence mixing coefficients. The distributed resistance model is adopted for modeling of momentum exchange between wire-wrapped fuel pin wall and fluid[13]. The transport of momentum and energy by turbulence diffusion across the subchannel volume boundaries was considered by the effective viscosity and conductivity. ASFRE was parallelized to enhance the computational performance for large-scale pin bundle analysis. For small-size 37-pin subassembly analysis, the computation performance is found to be improved by more than 60 times of the original version on CRAY-T3D (128 processor elements).

Code verification and validation were made using the data of the following out-of-pile experiments in both sodium and water with wire-wrapped pin bundles:

1) JOYO fuel subassembly mock-up test (128-pin bundle; water) for axial pressure drop,
2) MONJU fuel subassembly mock-up test (169-pin bundle; water) for axial pressure drop and circumferential pressure distribution along wrapper tube,
3) PLANDTL test (37-pin bundle; sodium) for coolant temperature fields in nominal operation condition[14],
4) CCTL-CFR test (61-pin bundle; sodium) for coolant temperature distribution under natural circulation condition[8], and
5) Scarlet-2 test (19-pin bundle; sodium) for coolant temperature distribution under partially flow-blocked condition (porous blockage)[15].

Each calculation result showed good agreement with experimental data. Numerical and experimental pressure drops are shown in *FIG. 17.* The experimental plots were from the water tests of 128-pin (Joyo) and 169-pin (Monju) bundles. These plots were traced well by ASFRE. Figure 18 shows comparison of temperature profiles in 37-pin subassemblies of PLANDTL. One can see that the computational error was slightly larger than uncertainty of the measurement.

The finite element analysis code SPIRAL is under development for predicting local characteristics of thermal-hydraulics behavior. The flow channel is descretized using second order isoparametric elements. This code will be used to evaluate the model parameters in the empirical correlations and offer detailed data for the engineering model verification of ASFRE. The present approach aims at substituting the mock-up experiment with the computer codes regarding thermal-hydraulic prediction of FBR fuel subassembly.

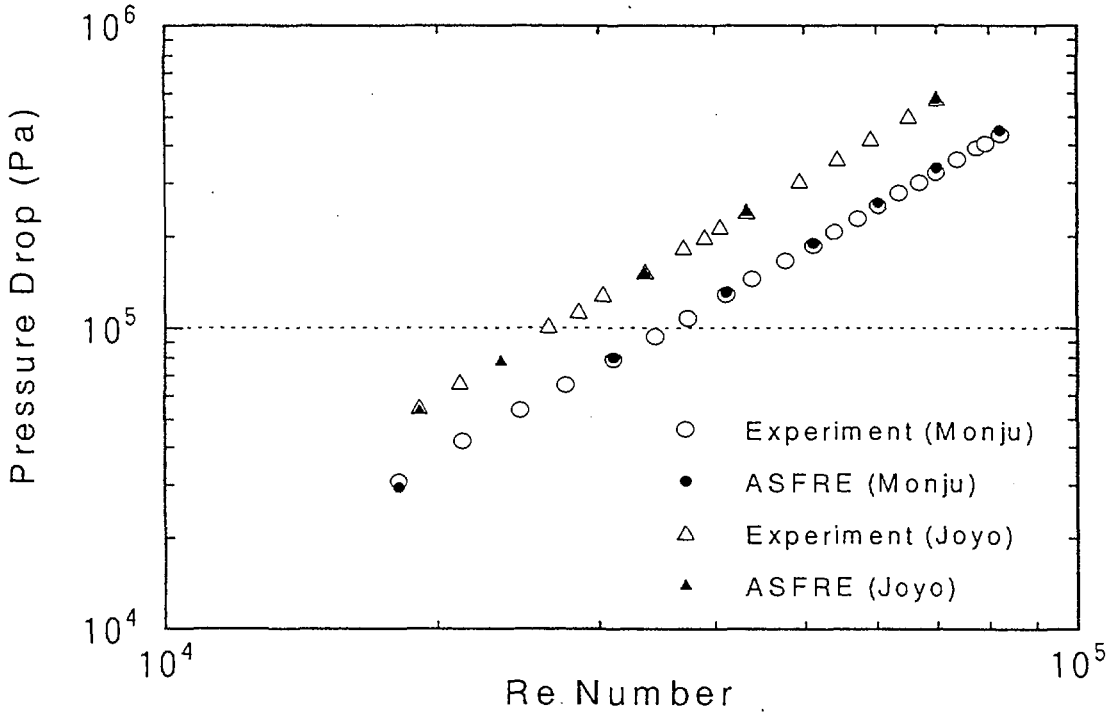

FIG. 17 Experimental and predicted pressure drop along modeled subassembly axis

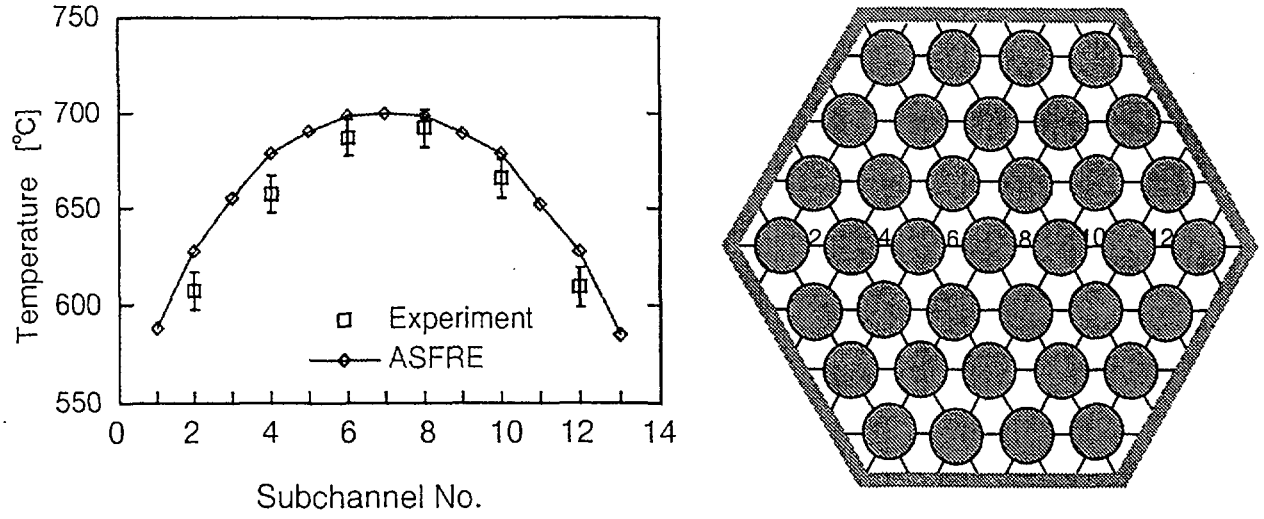

FIG. 18 Comparison of measured and predicted temperature profiles at the top end of heated section in the center subassembly of PLANDTL

4.2 Whole core thermal-hydraulic analysis code ACT

Whole core thermal-hydraulic analysis code ACT is being developed for the purpose of evaluating detailed in-core thermal hydraulic phenomena of fast reactors. For the high accurate predictive capability of the in-core thermal-hydraulics, key phenomena such as the IWF and core-plenum thermal-hydraulic interaction should be accounted for. Therefore, ACT consists of several thermal-hydraulic calculation modules related to the following regions:

1) subassemblies (fuel, blanket and control rods)
2) inter-subassembly gaps,

3) upper plenum and
4) primary heat transport system.

The subassembly module is almost equivalent to the subchannel analysis code ASFRE. The inter-subassembly gap module is used for calculating the flow and temperature fields in the gaps between the wrapper tubes (i.e. the IWF) and was also developed based on ASFRE code. The upper plenum and primary heat transport system modules are utilized to offer complicated boundary conditions to the whole-core analysis especially under natural circulation conditions with the operation of the direct reactor auxiliary coolant system. These four modules will be coupled with each other and be calculated simultaneously by using parallel computers.

The core model as the main part of ACT has been already developed by coupling the subassembly modules and the inter-subassembly gap module and it has made possible to calculate flow and temperature fields in the whole core including thermal interaction between the inner subassemblies and the inter-subassembly gaps. The coupling was made explicitly through the heat exchange on the wrapper tube outer surface from the viewpoints of flexibility to model various core geometry and program parallelization for large-scale simulation. The core model was applied to the analysis of PLANDTL-DHX sodium experiment whose test section consisted of 7 subassemblies for code verification. It was confirmed that the predicted sodium temperature distributions agreed with the measured data within the measurement error.

5. CONCLUSION

The overview was addressed on investigative activities of the fast reactor core thermal-hydraulics at PNC. The activities are mainly divided into three categories: Studies on natural circulation decay heat removal, local fault with blockage of porous media and advanced simulation codes. The status of these studies are summarized as follows.

1) Natural circulation decay heat removal
   - The numerical modeling was developed to predict thermal-hydraulic field in the subassemblies by introducing inter-subassembly mixing correlations. The modeling was validated thorough the analyses of steady and transient sodium experiment with and without inter-subassembly heat transfer. The numerical and experimental results agreed well showing that the modeling is capable of predicting the thermal-hydraulic field inside the subassembly.
   - The brick subassembly mesh arrangement was proposed to simulate the thermal interactions between inside and outside the subassemblies, especially featuring the IWF. This method could reproduce characteristics of the thermal-hydraulic field of the IWF.
2) Local fault with porous blockages
   - The strategic development has been carried out to establish a reliable evaluation method for predicting the hottest position and the highest temperature in the subassembly with porous blockages. The fundamental water test with 4-subchannel model and full-bundle with 37-pin water and sodium experiments have been performed to understand the phenomena in the subchannel scale and the subassembly scale. Also the multi-dimensional and subchannel analysis models have been developed. The multi-dimensional analysis gave useful information to understand blockage inside/outside interactions. The information from the experiments and the multi-dimensional analysis is used to derive lumped parameters and a model of porous blockage for the subchannel analysis.
3) Advanced codes for core thermal-hydraulics
   - The aims and strategies on the advanced codes development were presented. The ACT code based on subchannel code ASFRE is extended to perform whole core computation and under development to apply to the overall primary system dynamic calculation. The finite element code SPIRAL is also developed to carry out detailed simulations of the deformed bundles.

The sodium and water experiments will be performed continuously from now on to take thier advantages to develop the numerical modeling for the simulation codes. And detailed computations with the multi-dimensional codes will be also carried out to break down thermal-hydraulic phenomena

and complement the information acquired from the experiments to derive engineering models with lumped parameter for production runs of safety assessment using the codes such as ACT and ASFRE.

ACKNOWLEDGMENT

The authors are grateful to Mr. Kotake of JAPCO for useful discussion on the safety study and information on Japanese DFBR. And the authors appreciate Mr. Miyake of NDD Co. for his support for performing calculations and technicians of Joyo Sangyo Co. for their technical supports for the experiments.

REFERENCES

[1] M. Nishimura, H. Kamide, K. Hayashi and K. Momoi, "Inter-subassembly Heat Transfer During Natural Circulation Decay Heat Removal - Experimental Transient Behavior from Forced to Natural Circulation and its Multi-dimensional Analysis with Mixing Model -", Proc. of NURETH-8, Kyoto Japan, p.903, Oct. (1997).

[2] H. Ohshima and H. Ninokata, "Analysis of Thermal-Hydraulic Behavior in a Fast Reactor Fuel Subassembly with Porous Blockages," International Meeting on Advanced Reactor Safety (ARS'97), Orlando USA, (1997).

[3] Shih-Kuei Cheng, Tae Sun Ro and N. E. Todreas, "Energy Transfer Mechanism Under Mixed Convection Conditions in LMFBR Wire-Wrapped Bundles", Proc. of the 3rd Int. Topical Mtg. on Reactor Thermal Hydraulics, Newport USA, Oct. (1985).

[4] Shih-Kuei Cheng and Neil E. Todreas, "Hydrodynamic Models and Correlations For Bare and Wire-Wrapped Hexagonal Rod Bundles - Bundle Friction Factors, Subchannel Friction Factors and Mixing Parameters", Nuclear Engineering and Design, Vol. 92, pp.227-251, (1986).

[5] T. Muramatsu, "Development and application of multi-dimensional thermohydraulic code AQUA", PNC Technical Review, No. 76, Power reactor and nuclear fuel development corporation, Japan, (1990).

[6] H. Kamide, K. Hayashi and K. Momoi, "Experimental Study of Core Thermohydraulics in Fast Reactors during Transition from Forced to Natural Circulation - Influence of Inter-Wrapper Flow -", Proc. of NURETH-8, Kyoto Japan, p.922, Oct. (1997).

[7] C. Betts, M. W. Ashton, et al, "European Studies on Fast Reactor Core Interwrapper Flows", Proc. of FR'91, Kyoto Japan, p.1.15-1, Oct. (1991).

[8] H. Kamide, et al., "Inter-subassembly heat transfer during natural circulation decay heat removal of FBRs", Proc. of ICONE-3, Kyoto, Japan, S101-3, April (1995).

[9] T. S. Ro et al, "Porous Body Approach for Wire-wrapped rod bundle analysis", Proc.3rd International Topical Meeting on Nuclear Power Plant Thermal Hydraulics and Operations, Seoul, South Korea, Nov.,(1988).

[10] M. Tanaka, J. Kobayashi, T. Isozaki, M. Nishimura and H. Kamide, "An Experimental Investigation on Heat Transfer in a Subchannel with a Porous Blockage - The Influence of Flow on Temperature Distribution inside the Porous Blockage -", Proc of 5th ASME/JSME Thermal Engineering Joint Conference, (in preparation).

[11] D.R. Liles and W.H. Reed, "A Semi-Implicit Method for Two-Phase Fluid Dynamics", J. Comp. Phys., 26, 390, (1978).

[12] J.A. Meijerink and H.A. van der Vorst, "Guidelines for the Usage of Incomplete Decompositions in Solving Sets of Linear Equations as They Occur in Practical Problems", J. Comp. Phys., 44, 134, (1981).

[13] H. Ninokata, A. Efthimiadis, N. E. Todreas, "Distributed Resistance Modeling of Wire-wrapped Rod Bundles", NED, 104, pp.93-102, (1987)

[14] H. Hayafune, et al., "Out-of-Pile Experiment for Sodium Boiling in FBR Fuel Assembly", D15, 1993 Spring Mtg. of Atomic Energy Society of Japan, (1993).

[15] J. Olive and P. Jolas, "Internal Blockage in a Fissile Super-Phenix Type Subassembly: The Scarlet Experiments and Their Interpretation by The Cafca-NA3 Code", Nucl. Energy, 4, 287, (1990).